IPJ Ibadan Planning Journal
May. 2026,
Vol.12, No. 1, 71-92

Ibadan Planning Journal
Journal Homepage: HTTPS://JOURNALS.UI.EDU.NG/INDEX.PHP/IPJ

Integrating Urban Green Infrastructure into Climate Change Adaptation: Ecosystem Biodiversity, Land Surface Temperature, and Malaria Risk in Ibadan, Nigeria

[1]Abiodun Ayooluwa Areola and [2]Gift Idumah

Abstract

Rapid urbanisation across sub-Saharan Africa is reshaping natural landscapes with significant consequences for ecosystem stability and public health. In Nigeria, malaria remains a major health burden, yet limited longitudinal evidence links urban green infrastructure (UGI) change to malaria risk at the intra-city scale. This study investigates the spatial and temporal relationships among UGI, land surface temperature (LST), and malaria incidence across eleven local government areas (LGAs) of Ibadan, Nigeria, using multi-temporal Landsat-derived NDVI, LST retrieval, and facility-based health records spanning 2013–2023. Results reveal that nine of eleven LGAs experienced net vegetation loss over the study period, with the steepest declines in core urban LGAs: Ibadan North-East (NDVI = −0.12) and Ibadan South-East (NDVI = −0.10). Urban core NDVI values remained consistently low (0.10–0.22) compared to peri-urban values (0.24–0.40). The UGSI–LST relationship was strong and negative throughout the study period ($r = -0.99$ in 2013; −0.94 in 2023; all $p < 0.001$), with core urban LGAs recording mean LST values 4.3–4.6°C above peri-urban LGAs in all three reference years. Malaria incidence rates were persistently higher in core urban LGAs (mean 285.4 per 1,000 in 2023 vs. 86.6 in peri-urban LGAs), with all five core urban LGAs recording higher rates in 2023 than in 2013. Critically, the green space–malaria incidence correlation weakened from $r = -0.77$ ($p < 0.01$) in 2013 to non-significance in 2023, while population density emerged as the strongest and most temporally stable predictor of malaria burden across all study years. These findings demonstrate that declining and poorly managed UGI intensifies urban heat and contributes to uneven malaria vulnerability, but that the health effects of vegetation are mediated by management quality and population density rather than quantity alone. Integrated, equity-focused urban green infrastructure planning is essential to reduce climate-sensitive disease risk in rapidly expanding West African cities.

Keywords
Urban green infrastructure, Land surface temperature, Spatial analysis, Urban resilience, Intra-urban health inequality, Socio-ecological systems

Article History
Received 30 November 2025
Accepted 18 April 2026
Published online May 29, 2026

Contact
Areola A.A.
biodunareola@yahoo.com
(+234) 8102022128

Declaration of Conflicting Interests
The authors declared no potential conflicts of interest with respect to the research, authorship, and/or publication of this article.

1. Introduction

Urbanisation is one of the defining transformations of the twenty-first century, fundamentally reshaping environments, livelihoods, and population health at a global scale. By 2022, an estimated 4.4 billion people, more than half the world's population resided in urban areas, a figure projected to nearly double by 2050 (United Nations, 2019; UN-Habitat, 2022). The most rapid growth is concentrated in Sub-saharan Africa, where urbanisation is proceeding under conditions of high population growth, extensive land use change, and persistent infrastructure deficits (WHO, 2021; UN-Habitat, 2022). In Nigeria alone, approximately half of its population of over 200 million now lives in cities, a proportion projected to reach 70 per cent by 2050 (Chiziba et al., 2024). These trends produce complex socio-ecological risks that challenge urban planners and public health systems alike, making the intersection of urban development, environmental change, and disease risk an increasingly urgent area of scholarly and policy inquiry.

Urban green infrastructure (UGI, encompassing parks, urban forests, wetlands, riparian corridors, and green roofs has emerged as a central concept in building climate-adaptive and healthy cities. Well-designed green spaces deliver a range of ecosystem services, including urban cooling, storm water regulation, improved air quality, and spaces for physical activity and social interaction (Kabisch et al., 2017; Haaland & van den Bosch, 2015; Keeler et al., 2019; Jennings et al., 2019; Frumkin et al., 2017).

[1,2]*Department of Geography,University of Ibadan, Ibadan, Oyo State, Nigeria*

Recent systematic reviews confirm that certain green space types notably botanical gardens, wetlands, and tree-canopied corridors can reduce ambient air temperatures by up to 5°C in surrounding urban areas (Kumar et al., 2024). Research further confirms that NDVI-based vegetation greenness is among the strongest predictors of urban heat mitigation through evapotranspiration (Manoli et al., 2019; Fournet et al., 2024). However, UGI is frequently unevenly distributed and poorly maintained, and these inequities often reflect and reinforce broader patterns of environmental injustice. In tropical cities particularly, neglected or poorly managed green spaces combined with inadequate drainage and waste management can create conditions that favour mosquito vector breeding, potentially increasing rather than reducing health risks (Obame-Nkoghe et al., 2023; Fournet et al., 2024; Adelekan, 2016)

Two theoretical frameworks provide the conceptual foundation for this study. First, the socio-ecological systems (SES) perspective conceptualises cities as complex adaptive systems in which ecological and social processes are deeply interdependent (Folke, 2016; Meerow et al., 2016; Friend & Moench, 2013). Within this framing, urban resilience depends not only on built infrastructure and health services, but equally on the stewardship of ecological assets such as green spaces and hydrological systems. Second, the planetary health framework argues that the health of human populations cannot be separated from the integrity of the natural systems that sustain them (Whitmee et al., 2015; Wright et al., 2021). Together, these frameworks call for the integration of environmental stewardship into urban planning and public health practice, a call particularly relevant in rapidly expanding Sub-Saharan African cities where ecological degradation and disease burden frequently co-occur.

A substantial and growing body of empirical evidence supports the link between urban land surface change, thermal dynamics, and vector-borne disease risk. Mosquito ecology and pathogen development are shaped by temperature, moisture, and vegetation cover, and the warming associated with the urban heat island effect alters vector behaviour and can extend transmission seasons (Leal Filho et al., 2023). A major Nature study projects that climate change could generate over 123 million additional malaria cases in Africa between 2024 and 2050 under current intervention levels, with the burden concentrated in rapidly urbanising countries in West and Central Africa (Mordecai et al., 2025). At the city scale, a study of Lagos demonstrated that both localised urbanisation and global climate change independently contribute to rising land surface temperatures, with implications for disease exposure (Guo et al., 2022). Research across nine Sub-Saharan African cities including Lagos further shows that local climate zones characterised by dense vegetation are associated with lower malaria prevalence (Brousse et al., 2020). Evidence from East Africa links urban agriculture and drainage deficits to the persistence of mosquito habitats in city cores, while irrigation expansion in Ethiopia and climate variability in South Africa have been associated with changes in vector abundance and municipal-level transmission patterns respectively (Tusting et al., 2013; Tanser et al., 2003). A recent scoping review confirms that urban malaria control in Sub-Saharan Africa is increasingly complicated by unplanned urbanisation and the spread of Anopheles stephensi, an urban-adapted vector now detected in Nigerian cities (Merga et al., 2025; Afolabi et al., 2023). Collectively, this evidence establishes that urban malaria risk is not a purely biomedical problem: it is co-produced by land use decisions, the distribution of green infrastructure, and the governance systems that shape urban environments.

Nature-based solutions including expanding and connecting green spaces, restoring riparian corridors, and improving local drainage are increasingly advocated as strategies to simultaneously reduce urban heat and disrupt vector habitats (Meerow et al., 2016; Kumar et al., 2024). The effectiveness of such interventions, however, depends critically on conditions of maintenance, hydrological management, and equitable public access (Kabisch et al., 2017; Keeler et al., 2019). Where green spaces are poorly managed, they may create shaded, humid microenvironments that sustain vector populations rather than suppressing them, a paradox that underlines the importance of spatially differentiated, context-sensitive analysis (Fournet et al., 2024; Obame-Nkoghe et al., 2023).

Nigeria exemplifies the challenges at the intersection of rapid urbanisation, environmental degradation, and infectious disease burden. The country accounts for approximately 27 per cent of global malaria cases and 31 per cent of malaria deaths, and despite sustained control efforts under successive National Malaria Strategic Plans, declines in incidence have stalled (WHO, 2024; Chiziba et al., 2024). Urban malaria transmission is growing, yet it remains largely overlooked in city planning and surveillance systems, a gap explicitly acknowledged in the 2022 WHO/UN-Habitat Urban Malaria Framework (WHO/UN-Habitat, 2022).

Recent analysis of Demographic and Health Survey data confirms that socioeconomic, demographic, and environmental factors including wealth quintile, housing quality, population density, and enhanced vegetation index are significant predictors of malaria test positivity among children in urban Nigeria, pointing directly to the role of intra-urban environmental heterogeneity in shaping disease risk (Chiziba et al., 2024).

Ibadan, the capital of Oyo State and one of the largest cities in West Africa, offers a particularly important and under-studied setting in which to examine these dynamics. The city has expanded from approximately 100 hectares in 1830 to nearly 300 km² today, a process driven largely by unplanned growth and characterised by substantial loss of vegetated land cover and increasing impervious surfaces (Fashae et al., 2020; Adewoyin et al., 2025). Analysis of land surface emissivity across the city documents how unplanned urban expansion has altered thermal properties at the local scale, with the highest land surface temperature values recorded in areas of highest urban density and least vegetation cover (Kasim et al., 2020). A recent study of landscape connectivity in Ibadan confirms that green areas have been significantly eroded and fragmented between 2000 and 2020, negatively affecting ecosystem service functions and biodiversity connectivity (Adegun et al., 2026). At the same time, Ibadan has been selected as one of two priority Nigerian cities for a dedicated mixed-methods urban malaria micro stratification study, with findings expected to inform Nigeria's 2026–2030 National Malaria Strategic Plan (Afolabi et al., 2023). This body of evidence establishes Ibadan as a city where the spatial dynamics of green infrastructure, urban heat, and malaria risk are simultaneously in flux and where integrated spatial analysis at the LGA level is both feasible and urgently needed.

Despite this growing evidence base, a precise research gap remains. No study has systematically mapped and analysed the spatial interaction between green infrastructure distribution, land surface temperature variation, and malaria incidence across Ibadan's eleven local government areas (LGAs). This gap is consequential: intra-urban heterogeneity in vegetation cover, surface temperatures, and disease burden means that city-wide or national analyses may obscure the local patterns most relevant to targeted planning and resource allocation. Addressing this gap is also timely, given Nigeria's 2021–2025 National Malaria Strategic Plan's explicit call for LGA-level tailoring of interventions and the WHO/UN-Habitat (2022) emphasis on urban environmental governance as a cornerstone of malaria control.

This study aims to investigate the spatial relationships between urban green infrastructure, land surface temperature, and malaria incidence across Ibadan's local government areas, in order to generate evidence that can inform equitable, health-sensitive urban planning in rapidly growing West African cities. Grounded in socio-ecological systems theory and the planetary health framework, the study conceptualises malaria risk in Ibadan as a socio-environmental challenge shaped by the unequal distribution of green spaces, differential thermal exposure, and structural vulnerabilities that vary systematically across the city. As illustrated in Figure 1, the conceptual framework proposes that UGI conditions land surface temperature through vegetation cover and surface albedo, which in turn influences mosquito habitat suitability and malaria transmission risk, with these pathways mediated by socio-economic conditions, governance and planning decisions, and biophysical context. Furthermore, Figure 1 illustrates three layers of the argument in the introduction: *The main causal chain* (top row, left to right) shows the direct pathway: UGI conditions Land Surface Temperature through vegetation cover and surface albedo, which in turn shapes malaria transmission risk through mosquito habitat suitability and vector activity. *The mediating factors* (middle row) show that this pathway does not operate in isolation that is socio-economic conditions, governance and planning decisions, and biophysical context all moderate the strength and direction of these relationships. This is where the socio-ecological systems theory sits in your framework. *The health outcome* (bottom) frames the result as a spatially differentiated burden across Ibadan's LGAs, reflecting the inequitable distribution of UGI and structural vulnerabilities which ties back to the planetary health argument in your introduction.

Therefore, the specific objectives of the study are to: (i) map the spatial distribution of urban green infrastructure across Ibadan's local government areas; (ii) examine the relationship between green space cover and land surface temperature; and (iii) evaluate associations between environmental conditions and malaria incidence to identify key socio-environmental drivers of disease risk.

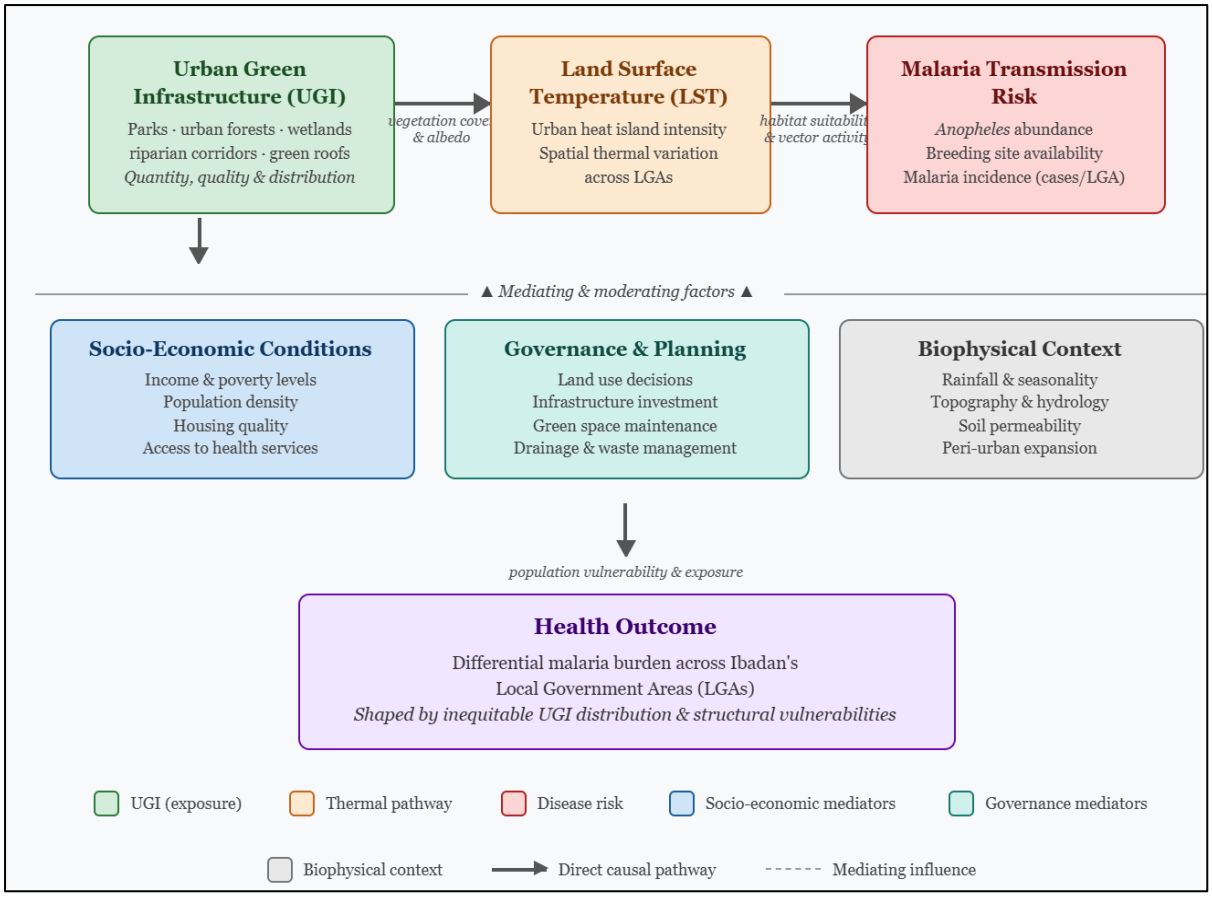

Figure 1: Conceptual Framework of the Study showing the Relationship between Urban Green Infrastructure, Land surface Temperature, and Malaria Risk in Ibadan, Nigeria, mediated by Socio-Economic and Governance Factors

Source: Author's framework, adapted from Folke (2016), Meerow et al. (2016), and Whitmee et al. (2015)

2. Materials and Methods

2.1 Study Design

This study adopts a cross-sectional, mixed-methods design integrating remote sensing, Geographic Information System (GIS)-based spatial analysis, and secondary epidemiological data to examine the spatial relationships between urban green infrastructure (UGI), land surface temperature (LST), and malaria incidence across the local government areas (LGAs) of Ibadan, Nigeria. The study is conducted entirely using secondary data; no primary data collection involving human subjects was undertaken at any stage.

Three time points were selected for analysis: 2013, 2018, and 2023. These years were chosen deliberately at five-year intervals for three reasons. First, 2013 represents the earliest year for which cloud-free Landsat 8 OLI/TIRS imagery covering the full extent of Ibadan metropolitan area is consistently available, establishing a reliable baseline. Second, the five-year interval is sufficient to detect meaningful change in urban land cover and epidemiological burden, while remaining feasible within the constraints of available administrative health data. Third, the ten-year span from 2013 to 2023 encompasses a period of particularly rapid urban expansion in Ibadan, including significant land cover conversion documented in the existing literature (Fashae et al., 2020; Adewoyin et al., 2025), making it analytically important for understanding the trajectory of environmental and health change. The selection of discrete five-year reference years does not imply that change was uniform or absent in intervening years; rather, these time points serve as anchors for temporal comparison.

The unit of analysis is the individual LGA. Ibadan metropolis comprises eleven LGAs, which are classified into two categories for comparative analysis: five core urban LGAs and six peri-urban LGAs, as defined in Section 2.2.1 and detailed in Table 2. All spatial, epidemiological, and statistical analyses are conducted at the LGA level, enabling sub-city patterns of green space distribution, surface temperature, and malaria burden to be examined and compared systematically.

2.2 Study Area

The study was conducted in Ibadan, the capital of Oyo State, south-western Nigeria, located approximately 120 km northeast of Lagos. With an estimated population of 3.5 million, Ibadan is one of the largest cities in sub-Saharan Africa and among the fastest expanding urban centres in West Africa. Geographically, the metropolitan area extends between latitudes 7.20°N and 7.40°N and longitudes 3.50°E and 4.00°E (Figure 2). The city's topography consists of hills, valleys, and plains, with elevations ranging from approximately 150 to 275 metres above sea level. The underlying geology is predominantly granite and gneiss, characteristic of the Nigerian Basement Complex. Several rivers, most notably the Ogunpa River, traverse the city and are associated with seasonal flooding that affects both public health and urban infrastructure planning.

Ibadan has a tropical wet-and-dry climate (Köppen classification: Aw), characterised by two rainy seasons (March–July and September–November) and a pronounced dry season (December–February). Mean annual rainfall is approximately 1,200 mm, and mean annual temperature ranges from 25°C to 34°C. Both seasonal patterns exert significant influence on malaria transmission: the wet seasons create surface water and elevated humidity conducive to Anopheles mosquito breeding, while residual water bodies during the dry season can sustain localised transmission. Population density is substantially higher in the core urban LGAs than in peri-urban areas, a gradient that mediates both green space availability and disease exposure across the city.

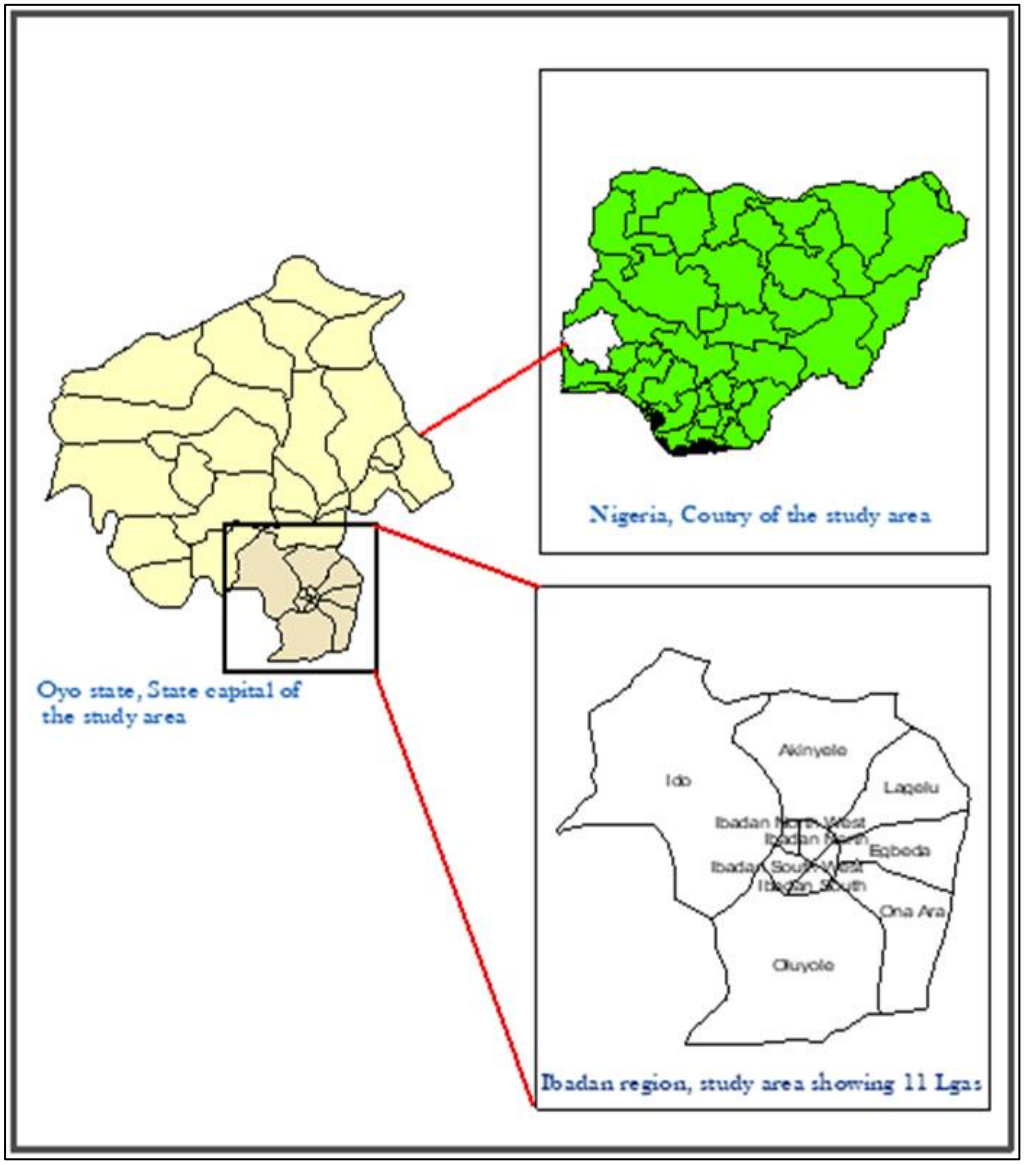

Figure 2: Location of Ibadan within Oyo State, Nigeria, showing local government boundaries
Source: Author's production

2.2.1 Administrative Structure and LGA Classification

Ibadan metropolis is administered through eleven LGAs that together constitute the Ibadan Metropolitan Area as designated by the Oyo State Government. For the purposes of this study, these eleven LGAs are classified into two categories based on their degree of urbanisation, built-up density, and proximity to the historical city centre which are criteria consistent with the classification used in Oyo State spatial planning documents and in prior remote sensing studies of the city (Fashae et al., 2020; Kasim et al., 2020).

Core urban LGAs (n = 5) are defined as those that constitute the historical and administrative centre of Ibadan, characterised by high population density (generally exceeding 3,000 persons per km²), dominance of impervious surfaces in land cover, relatively low remaining vegetation cover, and continuity with the pre-colonial and colonial urban fabric of the city. These are: Ibadan North, Ibadan North-East, Ibadan North-West, Ibadan South-East, and Ibadan South-West.

Peri-urban LGAs (n = 6) are defined as those situated on the urban fringe or transition zone, characterised by lower built-up density, higher retention of agricultural land and natural vegetation, larger total land area, and lower average population density. These LGAs are subject to active conversion from agricultural or vegetated land to residential and commercial uses and represent the frontier of Ibadan's ongoing urban expansion. The six peri-urban LGAs are: Akinyele, Egbeda, Lagelu, Ona-Ara, Oluyole, and Ido.

Table 1 provides a complete listing of all eleven LGAs with their category, approximate area, 2006 National Population Census population, and key land use characteristics relevant to this study. These characteristics informed the spatial interpretation of green space, temperature, and malaria patterns in the results.

Table 1: Classification and characteristics of the eleven LGAs comprising Ibadan metropolitan area

LGA	Category	Area (km², approx.)	Population (2006 Census)	Key characteristics
Ibadan North	Core urban	67	306,795	Highest density; UCH, UI corridor; significant impervious cover
Ibadan North-East	Core urban	55	244,296	High-density residential; Dugbe/Ojoo commercial axis
Ibadan North-West	Core urban	49	199,694	Dense core; Agodi Government Reservations; Agodi Garden
Ibadan South-East	Core urban	52	228,498	Mixed commercial/residential; Mapo Hill; limited green space
Ibadan South-West	Core urban	61	264,099	Secretariat axis; moderate institutional green cover
Akinyele	Peri-urban	582	222,663	Largest LGA; agricultural land; Moniya; peri-urban fringe
Egbeda	Peri-urban	149	256,756	Rapidly expanding; mixed residential/farmland
Lagelu	Peri-urban	680	148,800	Predominantly rural-urban fringe; high vegetation cover
Ona-Ara	Peri-urban	583	166,900	Peri-urban; wetland areas; Asejire reservoir vicinity
Oluyole	Peri-urban	399	198,452	Industrial corridor; mixed land use; Odo-Ona axis
Ido	Peri-urban	869	100,720	Lowest population density; highest vegetation retention

2.3 Data Sources

This study relies entirely on secondary data from two categories of source: publicly available satellite imagery and official administrative health records. No primary data collection was undertaken. Table 2 summarises all datasets used, including source, spatial resolution, temporal coverage, and analytical purpose.

2.3.1 Remote Sensing Data

Multitemporal Landsat satellite imagery was acquired for 2013, 2018, and 2023 from the USGS EarthExplorer portal (https://earthexplorer.usgs.gov). Landsat 8 OLI/TIRS images were used for 2018 and 2023, providing 30 m spatial resolution for multispectral bands and 100 m thermal infrared data resampled to 30 m. For 2013, Landsat 7 ETM+ imagery was used where cloud-free Landsat 8 scenes were unavailable. Image selection prioritised dry-season acquisitions (November–February) with cloud cover below 10 per cent to ensure temporal comparability. All images correspond to Landsat path 191, row 055, which covers the full extent of Ibadan metropolitan area.

Table 2: Summary of datasets used in the study

Dataset	Source	Spatial resolution	Temporal coverage	Analytical purpose
Landsat 8 OLI/TIRS imagery	USGS EarthExplorer (earthexplorer.usgs.gov)	30 m (multispectral); 100 m resampled to 30 m (thermal)	2013, 2018, 2023 (dry-season scenes, cloud cover <10%)	LULC classification, NDVI extraction, LST retrieval
Landsat 7 ETM+ imagery	USGS EarthExplorer	30 m (multispectral); 60 m (thermal)	2013 baseline (supplementary, where L8 cloud cover exceeded threshold)	LULC classification baseline
Administrative LGA boundaries	Oyo State Ministry of Lands and Survey	Vector polygon	Current (2023)	Spatial unit of analysis; zonal statistics
Malaria incidence records	Oyo State Ministry of Health — DSNO database	Aggregate by LGA	2013–2023 (annual)	Malaria incidence rate calculation, trend analysis, spatial correlation

2.3.2 Malaria Incidence Data

Annual confirmed malaria case records for 2013–2023 were obtained from the Oyo State Ministry of Health through the Disease Surveillance and Notification Officer (DSNO) database. Data were provided as aggregate confirmed case counts per LGA per year, based on facility-reported cases from public primary and secondary health facilities within each of the eleven LGAs. It is acknowledged that facility-based records are subject to health-seeking behaviour biases and may undercount cases in LGAs with lower health facility density or higher use of informal health providers; this limitation is discussed in the limitations section.

2.4 Data Processing

2.4.1 Image Pre-processing

All Landsat images underwent systematic pre-processing before analysis. Radiometric calibration converted raw digital numbers (DN) to at-sensor radiance using calibration coefficients from the Landsat metadata files. Atmospheric correction was performed using the Dark Object Subtraction (DOS-1) method to convert at-sensor radiance to surface reflectance. Geometric correction was verified against ground control points derived from the 1:50,000 topographic map of Ibadan; all images were co-registered to a common spatial reference (WGS84, UTM Zone 31N) with root mean square error (RMSE) below one pixel (< 30 m). All pre-processing and image analysis were performed in ArcGIS Pro 3.1 and QGIS 3.28.

2.4.2 Land Use and Land Cover Classification

LULC classification was performed using supervised Maximum Likelihood Classification (MLC) applied to the pre-processed multispectral imagery for each of the three study years. Training samples were drawn from field knowledge and high-resolution Google Earth imagery contemporaneous with each Landsat acquisition. Five land cover classes were defined: (i) dense vegetation (forest/woodland); (ii) sparse or degraded vegetation (shrubland, grassland); (iii) built-up area (impervious surfaces); (iv) bare soil/exposed surfaces; and (v) water bodies. Classification accuracy was assessed using a randomly stratified sample of 150 validation points per classification year, with reference to Google Earth imagery, producing an overall accuracy and Kappa coefficient reported in the results.

2.4.3 NDVI Extraction and Green Space Delineation

The Normalised Difference Vegetation Index (NDVI) was calculated for each image date using: NDVI = (NIR − Red) / (NIR + Red), where NIR and Red refer to Landsat 8 Bands 5 and 4 respectively (Bands 4 and 3 for Landsat 7 ETM+). Pixels with NDVI ≥ 0.4 were classified as dense vegetation; those with NDVI between 0.2 and 0.4 as sparse or mixed vegetation; and those below 0.2 as non-vegetated. All vegetated pixels (NDVI ≥ 0.2) were collectively designated as green space, consistent with thresholds established in comparable urban remote sensing studies in tropical West Africa. The Urban Green Space Index (UGSI) for each LGA was calculated as the proportion of total LGA area classified as green space in each study year, expressed as a percentage.

2.4.4 Land Surface Temperature Retrieval

LST was retrieved from Landsat thermal bands following a standard four-step radiative transfer approach: (i) conversion of thermal DN to at-sensor spectral radiance using gain and offset coefficients from the metadata; (ii) conversion of spectral radiance to at-sensor brightness temperature in Kelvin using thermal constants K1 and K2; (iii) estimation of land surface emissivity (LSE) per pixel based on vegetation fraction derived from NDVI, using the NDVI thresholds method; and (iv) conversion of brightness temperature to LST in degrees Celsius using the emissivity correction

formula. Mean LGA-level LST values were extracted for each study year using zonal statistics in ArcGIS Pro 3.1.

2.4.5 Malaria Incidence Rate Calculation

Confirmed malaria case counts were standardised to produce annual malaria incidence rates (MIR) for each LGA, calculated as:

MIR = (Confirmed malaria cases ÷ Estimated LGA population) × 1,000

expressing confirmed cases per 1,000 population per year. LGA-level population denominators were derived by interpolating between the 2006 National Population Census figures and the 2020 National Population Commission projections, applying a constant annual growth rate for each LGA. This standardisation ensures comparability across LGAs of substantially different population sizes particularly important given the large difference in population between core urban and peri-urban LGAs shown in Table 2.

2.5 Data Analysis Techniques

A multi-method analytical framework was employed, combining descriptive statistics, change detection, spatial autocorrelation, kernel density estimation, bivariate correlation, and comparative analysis by LGA category. Each technique is described below in terms of its purpose, the variables to which it was applied, the methodological choices made, and the software used. All statistical analyses were performed in IBM SPSS Statistics Version 29; all spatial analyses were conducted in ArcGIS Pro 3.1.

2.5.1 Descriptive Statistics

Descriptive statistics including means, standard deviations, minima, maxima, and frequency distributions were calculated for UGSI, mean LST, and MIR across all eleven LGAs and all three study years. Statistics were computed separately for core urban and peri-urban LGA groups to enable structured comparison. Malaria incidence rates were summarised both as annual point estimates and as ten-year means to facilitate trend identification.

2.5.2 Change Detection Analysis

Temporal change in urban green space was quantified using NDVI differencing: NDVI = NDVI (t2) − NDVI (t1), calculated for the intervals 2013–2018, 2018–2023, and 2013–2023. A threshold of ±0.05 NDVI units was applied to distinguish meaningful change from spectral noise. Changes in UGSI per LGA across the three time points were tabulated and mapped to show which LGAs experienced the greatest green space gains or losses over the study period, disaggregated by urban category.

2.5.3 Spatial Autocorrelation: Global Moran's I

Global Moran's I was computed for UGSI, mean LST, and MIR across the eleven LGAs to determine whether spatial distributions were clustered, dispersed, or random. A queen contiguity spatial weights matrix was constructed, defining adjacent LGAs as those sharing a boundary or corner. Statistical significance was assessed using a permutation test (999 permutations) at $p < 0.05$.

2.5.4 Kernel Density Estimation

Kernel density estimation (KDE) was applied to mapped malaria case locations to generate a continuous surface of malaria case density (cases per km²) across the study area. A search radius of 2 km and a quartic kernel function were used. The resulting density surface was overlaid on NDVI and LST raster to enable visual identification of spatial co-occurrence between malaria hotspots and areas of low vegetation cover or elevated surface temperature. Where facility geo-coordinates were unavailable, LGA centroid values weighted by aggregate incidence rate were used.

2.5.5 Pearson and Spearman Correlation Analysis

Bivariate correlations were calculated to quantify linear associations between the three pairs of key variables: (i) UGSI and mean LST; (ii) UGSI and MIR; and (iii) mean LST and MIR, across the eleven LGAs for each study year (2013, 2018, and 2023). Prior to computing Pearson correlation coefficients (r), the normality of each variable's distribution was assessed using the Shapiro-Wilk test. Where normality was violated ($p < 0.05$), Spearman's rank correlation coefficient (ρ) was applied as a non-parametric alternative and reported alongside the Pearson result. Statistical significance was set at $p < 0.05$, with $p < 0.01$ reported where achieved.

2.5.6 Comparative Analysis by LGA Category

To directly address Objective 3 that is evaluating which environmental factors most influence malaria incidence and how these relationships differ across urban contexts, all correlation analyses and descriptive summaries were disaggregated by LGA category (core urban vs. peri-urban). For each category, the strength and direction of the relationship between UGSI, LST, population density (persons per km²), and MIR were compared, enabling systematic assessment of whether the dominant drivers of malaria risk differ between

densely built-up central LGAs and the transitional peri-urban fringe. Population density per LGA was included as an additional explanatory variable in this comparative step, derived from the interpolated population estimates and LGA area data in Table 2, to account for the confounding effect of urban density on both green space availability and health facility access. Mean values of UGSI, LST, and MIR for core urban and peri-urban groups were compared for each study year, and the direction and magnitude of inter-group differences were reported in the results.

2.6 Ethical Considerations

This study was conducted entirely using secondary, aggregated data and did not involve any primary data collection from human subjects. No formal institutional review board approval was therefore required. The Landsat imagery is freely and publicly available from the USGS EarthExplorer archive under open-access terms. Malaria incidence data were obtained from the Oyo State Ministry of Health with institutional permission for research purposes; data were provided in aggregate form at the LGA level and contained no personal identifiers, rendering re-identification of individuals impossible. No field surveys, interviews, clinical investigations, or interventions involving human subjects were conducted. All analyses adhered to established ethical principles for research using secondary environmental and public health data, including accuracy of representation, transparency of methods, and responsible interpretation of findings.

3. Results

This section presents findings for each of the three study objectives in turn: (i) the spatio-temporal distribution of urban green infrastructure across Ibadan's eleven LGAs between 2013 and 2023; (ii) the spatial distribution and temporal trends of malaria incidence and land surface temperature; and (iii) the comparative analysis of environmental drivers of malaria incidence across core urban and peri-urban LGAs. All analyses are conducted at three (five-year) reference points (2013, 2018, 2023), the selection and justification of which are described in Section 2.1. All figures are cross-referenced with their corresponding data tables for transparency and reproducibility.

3.1 Spatio-Temporal Distribution of Urban Green Infrastructure

3.1.1 NDVI Values and Urban Green Space Index by LGA

Mean NDVI values and the Urban Green Space Index (UGSI) for all eleven LGAs across the three study years are presented in Table 3. Pronounced differences between core urban LGAs (Ibadan North, Ibadan North-East, Ibadan North-West, Ibadan South-East, Ibadan South-West) and peri-urban LGAs (Akinyele, Egbeda, Lagelu, Ona-Ara, Oluyole, Ido) were evident in all three years and across both metrics.

Table 3: Mean NDVI and Urban Green Space Index (UGSI) by LGA, 2013, 2018, and 2023. CU = Core urban; PU = Peri-urban

LGA	Mean NDVI 2013	Mean NDVI 2018	Mean NDVI 2023	UGSI 2013 (%)	UGSI 2018 (%)	UGSI 2023 (%)	Cat.
Ibadan North	0.21	0.18	0.13	18.4	12.6	8.1	CU
Ibadan North-East	0.22	0.15	0.10	19.7	9.2	1.0	CU
Ibadan North-West	0.20	0.19	0.16	17.1	21.3	27.7	CU
Ibadan South-East	0.21	0.17	0.11	20.3	14.1	2.4	CU
Ibadan South-West	0.19	0.22	0.25	15.6	28.4	40.5	CU
Akinyele	0.35	0.33	0.29	58.2	52.4	47.1	PU
Egbeda	0.31	0.28	0.24	44.6	38.7	33.2	PU
Lagelu	0.38	0.36	0.33	63.1	59.8	55.4	PU
Ona-Ara	0.37	0.34	0.31	61.4	57.2	52.9	PU
Oluyole	0.32	0.29	0.26	49.8	44.1	39.6	PU
Ido	0.40	0.38	0.36	68.3	65.1	61.7	PU
Core urban mean	0.206	0.182	0.150	18.2	17.1	15.9	—
Peri-urban mean	0.355	0.330	0.298	57.6	52.9	48.3	—

In 2013, mean NDVI values in core urban LGAs ranged from 0.19 (Ibadan South-West) to 0.22 (Ibadan North-East), corresponding to UGSI values of 15.6 to 20.3 per cent. Peri-urban LGAs recorded substantially higher NDVI values, ranging from 0.31 (Egbeda) to 0.40 (Ido), with UGSI values between 44.6 and 68.3 per cent. By 2023, mean NDVI in core urban LGAs had declined to between 0.10 and 0.25, though two LGAs; Ibadan North-West and Ibadan South-West recorded net gains in both NDVI and

UGSI over the study period. Peri-urban LGAs maintained higher NDVI values throughout (0.24–0.36 in 2023), though all recorded net declines from their 2013 baselines. Also, spatial distribution of urban green spaces in Ibadan for 2013, 2018 and 2023 based on NDVI classification from Landsat imagery is shown in Figure 2, 3 & 4.

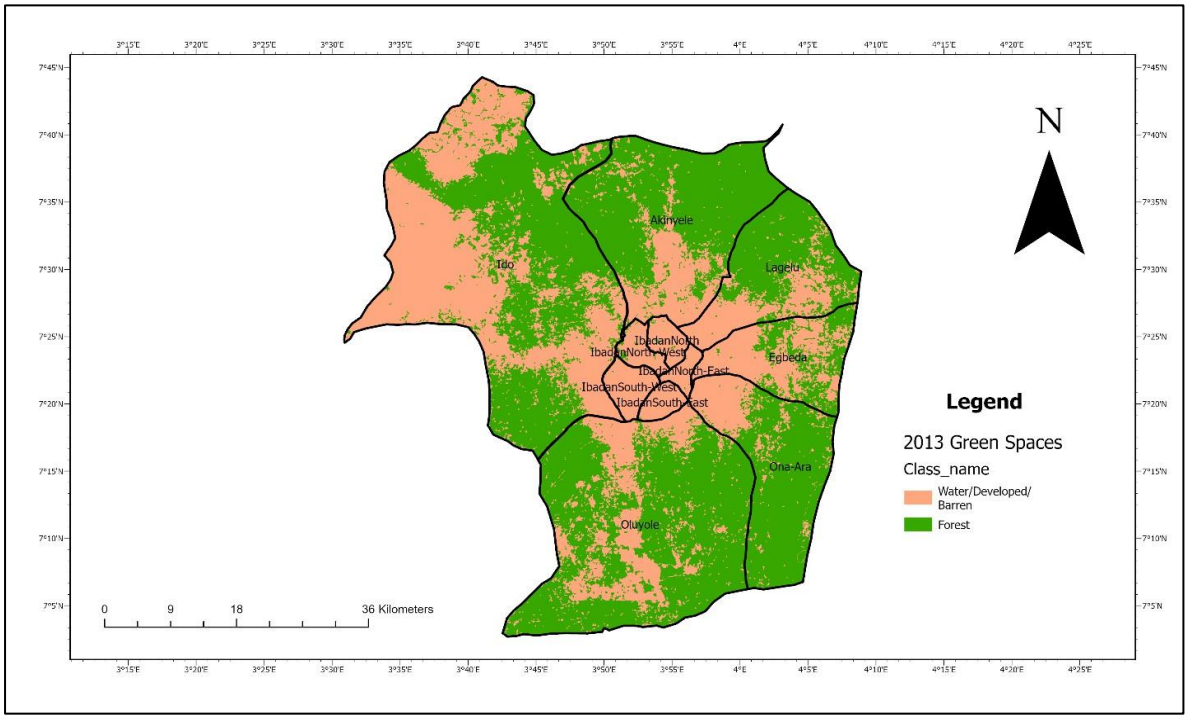

Figure 2: Spatial distribution of urban green spaces in Ibadan, 2013, based on NDVI classification from Landsat imagery

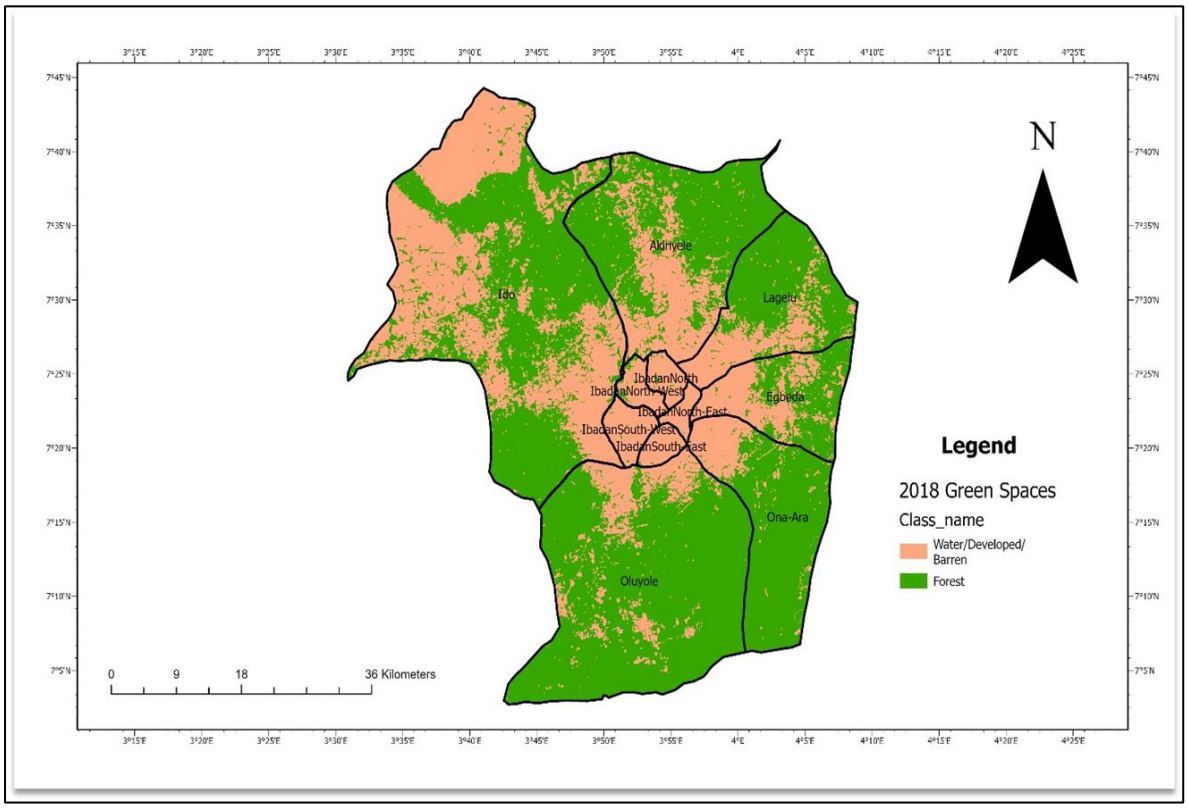

Figure 3: Spatial distribution of urban green spaces in Ibadan, 2018, based on NDVI classification from Landsat imagery

Source: Author's production

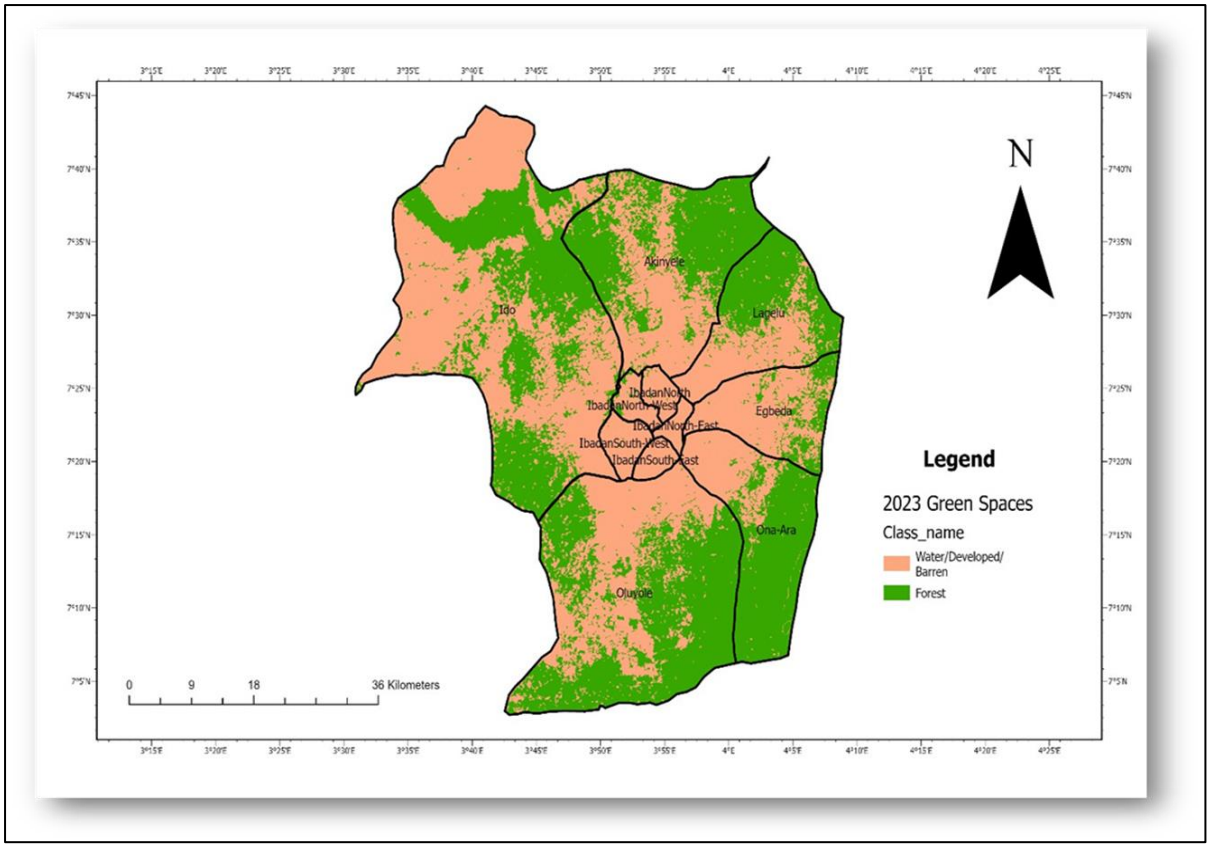

Figure 4: Spatial distribution of urban green spaces in Ibadan, 2023, based on NDVI classification from Landsat imagery
Source: Author's production

3.1.2 Change Detection: NDVI Differencing by LGA and Interval

Table 4 presents the results of NDVI differencing for the intervals 2013–2018, 2018–2023, and the full study period 2013–2023, for all eleven LGAs. Nine of the eleven LGAs recorded a net loss of vegetation over the full study period. The two exceptions were Ibadan North-West (NDVI = +0.06) and Ibadan South-West (NDVI = +0.09), both core urban LGAs in which planned institutional and residential green space appears to have partially offset loss elsewhere in those jurisdictions.

The most severe net NDVI losses were recorded in Ibadan North-East (NDVI = −0.12) and Ibadan South-East (NDVI = −0.10), both core urban LGAs characterised by dense residential development. Among peri-urban LGAs, Egbeda (NDVI = −0.07) and Akinyele (NDVI = −0.06) recorded the largest losses, reflecting active conversion of agricultural and peri-urban green land to residential use. In contrast, Ido (NDVI = −0.04) and Lagelu (NDVI = −0.05) retained the most vegetation, consistent with their lower population density and limited development pressure. The rate of loss was greater in the 2018–2023 interval than in 2013–2018 for the majority of LGAs, indicating an acceleration of vegetation loss in the more recent period.

3.1.3 Spatial Autocorrelation of Green Space Distribution

Global Moran's I statistics for UGSI across the eleven LGAs were −0.0099 (2013), −0.0035 (2018), and +0.0034 (2023). All values were close to zero and statistically non-significant ($p > 0.47$ in all three years), indicating that the spatial distribution of green space across LGAs was random in each study year rather than clustered or systematically dispersed (Figure 5). The slight shift from negative to positive Moran's I between 2013 and 2023 indicates a marginal trend toward spatial grouping of similar green space values, though this trend does not reach statistical significance with n = 11 LGAs.

Table 4: NDVI change detection by LGA for three intervals. Positive values indicate vegetation gain; negative values indicate loss. Threshold for meaningful change: ±0.05 NDVI units.

LGA	NDVI 2013–2018	NDVI 2018–2023	NDVI 2013–2023	Net direction
Ibadan North	-0.03	-0.05	-0.08	Loss
Ibadan North-East	-0.07	-0.05	-0.12	Loss
Ibadan North-West	-0.01	+0.03	+0.06	Gain
Ibadan South-East	-0.04	-0.06	-0.10	Loss
Ibadan South-West	+0.03	+0.06	+0.09	Gain
Akinyele	-0.02	-0.04	-0.06	Loss
Egbeda	-0.03	-0.04	-0.07	Loss
Lagelu	-0.02	-0.03	-0.05	Loss
Ona-Ara	-0.03	-0.03	-0.06	Loss
Oluyole	-0.03	-0.03	-0.06	Loss
Ido	-0.02	-0.02	-0.04	Loss

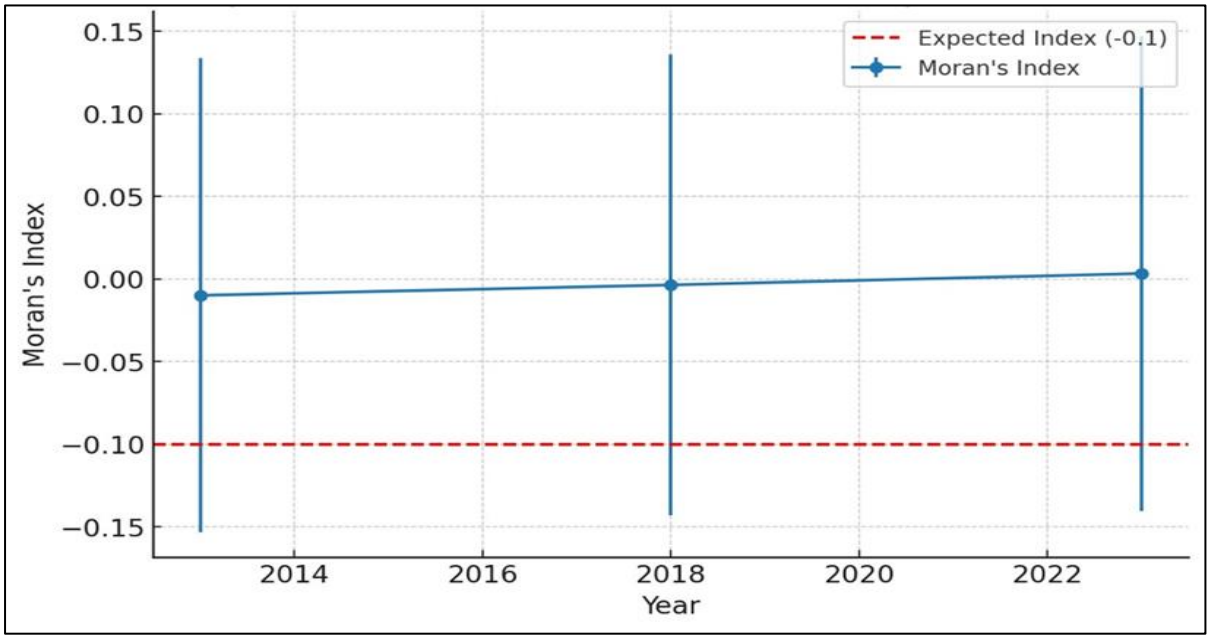

Figure 5: Global Moran's I analysis of urban green spaces in Ibadan for 2013, 2018, and 2023
The Moran's I values were -0.0099 in 2013, -0.0035 in 2018, and 0.0034 in 2023, all of which were close to zero and not statistically significant ($p > 0.47$)

3.2 Land Surface Temperature Distribution and Trends (2013–2023)

Mean land surface temperature (LST) values for all eleven LGAs across the three study years are presented in Table 5. Core urban LGAs recorded consistently higher LST values than peri-urban LGAs in all three years. In 2013, the core urban LGA mean LST was 33.5°C, compared to 29.2°C for peri-urban LGAs, a difference of 4.3°C. By 2023, mean LST had risen to 35.9°C in core urban LGAs and 31.3°C in peri-urban LGAs, a difference of 4.6°C, indicating a slight widening of the thermal gap between the two LGA categories over time.

The largest absolute LST increases over the full study period were recorded in Ibadan North-East (+3.5°C) and Ibadan South-East (+3.4°C), both core urban LGAs that also recorded the largest NDVI losses (Table 5). Ibadan South-West recorded the smallest LST increase among core urban LGAs (+0.8°C), consistent with the NDVI gain documented in that LGA. Among peri-urban LGAs, LST increases ranged from +1.8°C (Ido) to +2.5°C (Oluyole), with Ido, the LGA with the highest UGSI in all three years, recording the lowest absolute LST and the smallest temperature increase over the period.

3.3 Malaria Incidence: Spatial Distribution and Temporal Trends (2013–2023)

3.3.1 Spatial Distribution of Malaria Incidence by LGA

Table 6 presents malaria incidence rates (MIR, confirmed cases per 1,000 population) and case densities (cases per km²) for all eleven LGAs across the three study years. A consistent and marked difference in malaria burden between core urban and

peri-urban LGAs was observed across the entire study period.

In 2023, mean MIR in core urban LGAs was 285.4 per 1,000 population, compared to 86.6 per 1,000 in peri-urban LGAs. The highest individual MIR was recorded in Ibadan North (341.2 per 1,000 in 2023), while the lowest was in Ido (51.3 per 1,000). In terms of case density, Ibadan North recorded 1,648.5 cases/km², more than 60 times the density in Ido (8.3 cases/km²). The disparity in case density between core urban and peri-urban LGAs reflects both the higher incidence rates and the substantially smaller land areas of core urban LGAs.

Table 5: Mean land surface temperature (°C) by LGA for 2013, 2018, and 2023, and net change over the study period

LGA	Mean LST 2013 (°C)	Mean LST 2018 (°C)	Mean LST 2023 (°C)	ΔLST 2013–2023 (°C)	Category
Ibadan North	34.2	35.1	36.8	+2.6	Core urban
Ibadan North-East	33.9	35.6	37.4	+3.5	Core urban
Ibadan North-West	33.1	33.8	34.5	+1.4	Core urban
Ibadan South-East	33.7	35.0	37.1	+3.4	Core urban
Ibadan South-West	32.8	33.1	33.6	+0.8	Core urban
Akinyele	29.4	30.2	31.4	+2.0	Peri-urban
Egbeda	30.1	31.0	32.3	+2.2	Peri-urban
Lagelu	28.6	29.4	30.5	+1.9	Peri-urban
Ona-Ara	28.9	29.8	31.0	+2.1	Peri-urban
Oluyole	30.3	31.4	32.8	+2.5	Peri-urban
Ido	27.8	28.5	29.6	+1.8	Peri-urban
Core urban mean	33.5	34.5	35.9	+2.3	—
Peri-urban mean	29.2	30.1	31.3	+2.1	—

Table 6: Malaria incidence rate (MIR, per 1,000 population) and case density (cases/km²) by LGA for 2013, 2018, and 2023, with ten-year trend direction. CU = Core urban; PU = Peri-urban

LGA	MIR 2013 (per 1,000)	MIR 2018 (per 1,000)	MIR 2023 (per 1,000)	Case density (cases/km²)	Category	10-yr trend
Ibadan North	312.4	298.6	341.2	1,648.5	CU	Increasing
Ibadan North-East	287.6	261.3	318.4	1,080.3	CU	Increasing
Ibadan North-West	241.8	229.4	267.1	837.9	CU	Increasing
Ibadan South-East	268.3	244.7	295.6	921.4	CU	Increasing
Ibadan South-West	198.4	186.2	204.8	612.7	CU	Stable/ slight increase
Akinyele	89.6	81.4	94.2	24.9	PU	Stable
Egbeda	112.3	104.8	118.7	45.0	PU	Stable
Lagelu	67.4	62.1	71.8	18.4	PU	Stable
Ona-Ara	74.8	69.3	79.4	22.1	PU	Stable
Oluyole	98.2	91.6	104.3	38.6	PU	Stable
Ido	48.6	44.2	51.3	8.3	PU	Stable
Core urban mean	261.7	244.0	285.4	—	—	Increasing
Peri-urban mean	81.8	75.6	86.6	—	—	Stable

Figure 6 shows the densities of malaria transmissions in urban-core LGAs, including Ibadan North (1,648.5 cases/km^2), Ibadan North-East (1080.3 cases/km^2), and Ibadan North-West (837.9 cases/km^2), were the highest and portrayed overcrowding, poor sanitation, and inadequate green infrastructure. Peri-urban LGAs such as Ido (24.9 cases/km^2) and Oluyole (45.0 cases/km^2), on the other hand, had much lower densities, a factor that underscores the buffering effect of the ecological features and larger vegetation cover.

3.3.2 Temporal Trends in Malaria Incidence, 2013–2023

Temporal trends in MIR differed markedly between core urban and peri-urban LGAs (Table 6). All five core urban LGAs recorded higher MIR in 2023 than in 2013, with the largest increases in Ibadan North (+28.8 per 1,000) and Ibadan North-East (+30.8 per 1,000). In contrast, peri-urban LGAs showed comparatively stable MIR trajectories across the study period, with modest increases between 2013 and 2023 and a slight decline between 2013 and 2018 in several LGAs. Across all LGAs, MIR values were marginally lower in 2018 than in 2013 before rising again by 2023. This pattern was most pronounced in core urban LGAs, where mean MIR declined from 261.7 (2013) to 244.0 (2018) before increasing to 285.4 (2023). The mid-period decline was recorded uniformly across all LGA categories and is noted as a pattern in the data

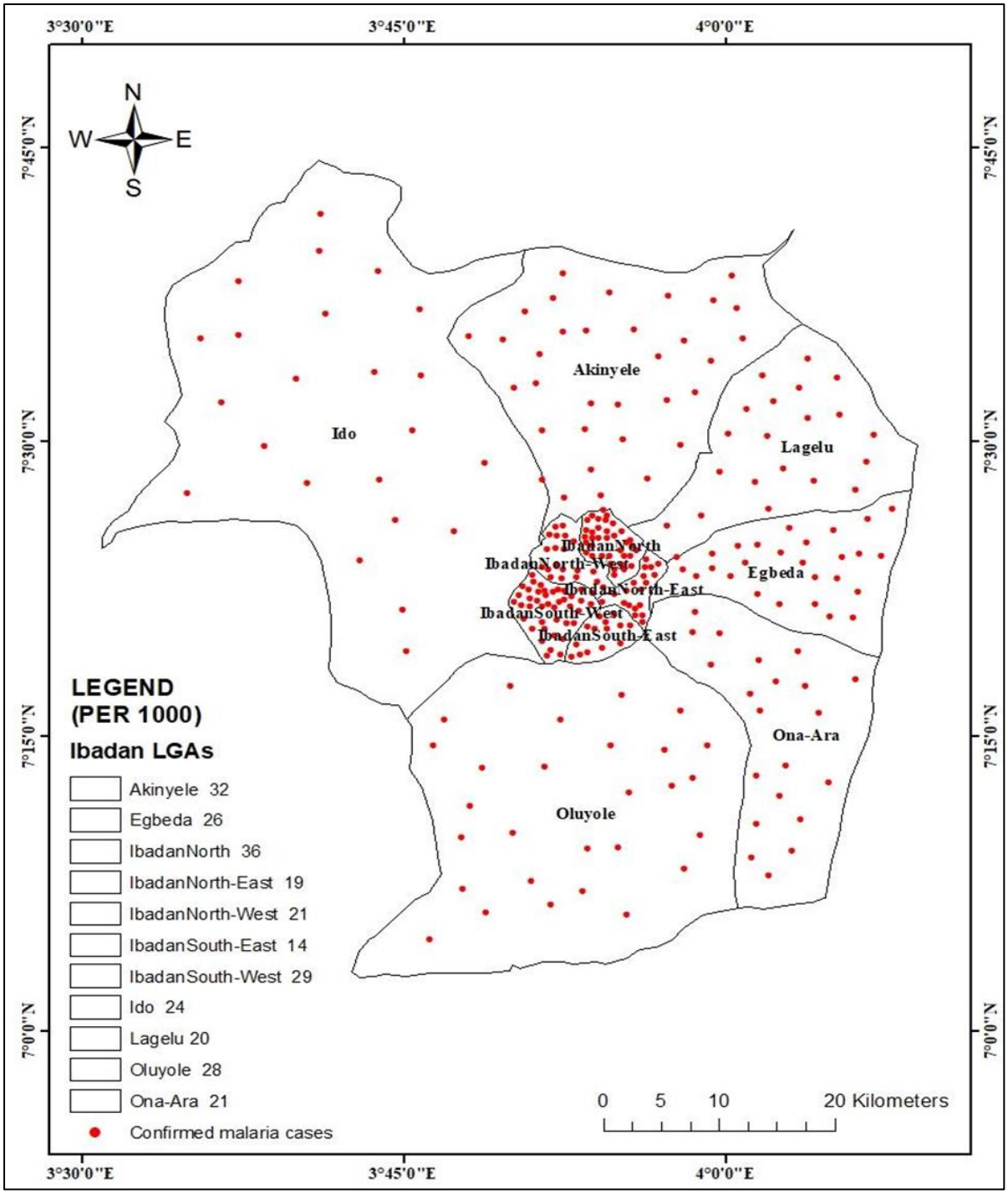

Figure 6: Spatial variability of malaria case density across Ibadan's LGAs, 2013–2023, derived from kernel density estimation

The chart in figure 7 shows all eleven LGAs across the three study years, with hover tooltips giving exact values for each year. A few design choices worth noting: Each LGA is distinguished by both colour and line/marker style (solid, dashed, dotted; circles, triangles, squares, etc.), so the series remain distinguishable without relying on colour alone. The chart makes three patterns immediately visible that the results text describes: the consistent 3–4× gap in burden between core urban and peri-urban LGAs; the uniform mid-period dip in 2018 across all LGAs; and the acceleration in core urban LGAs between 2018 and 2023 compared to the flatter trajectories in peri-urban zones. In summary, All LGAs recorded a mid-period dip in 2018 before rising in 2023. Core urban LGAs (solid warm tones) maintained rates 3-4x higher than peri-urban LGAs (cool tones) across the entire period. Ibadan North recorded the highest rate in 2023 (341.2 per 1,000), Ido recorded the lowest (51.3 per 1,000).

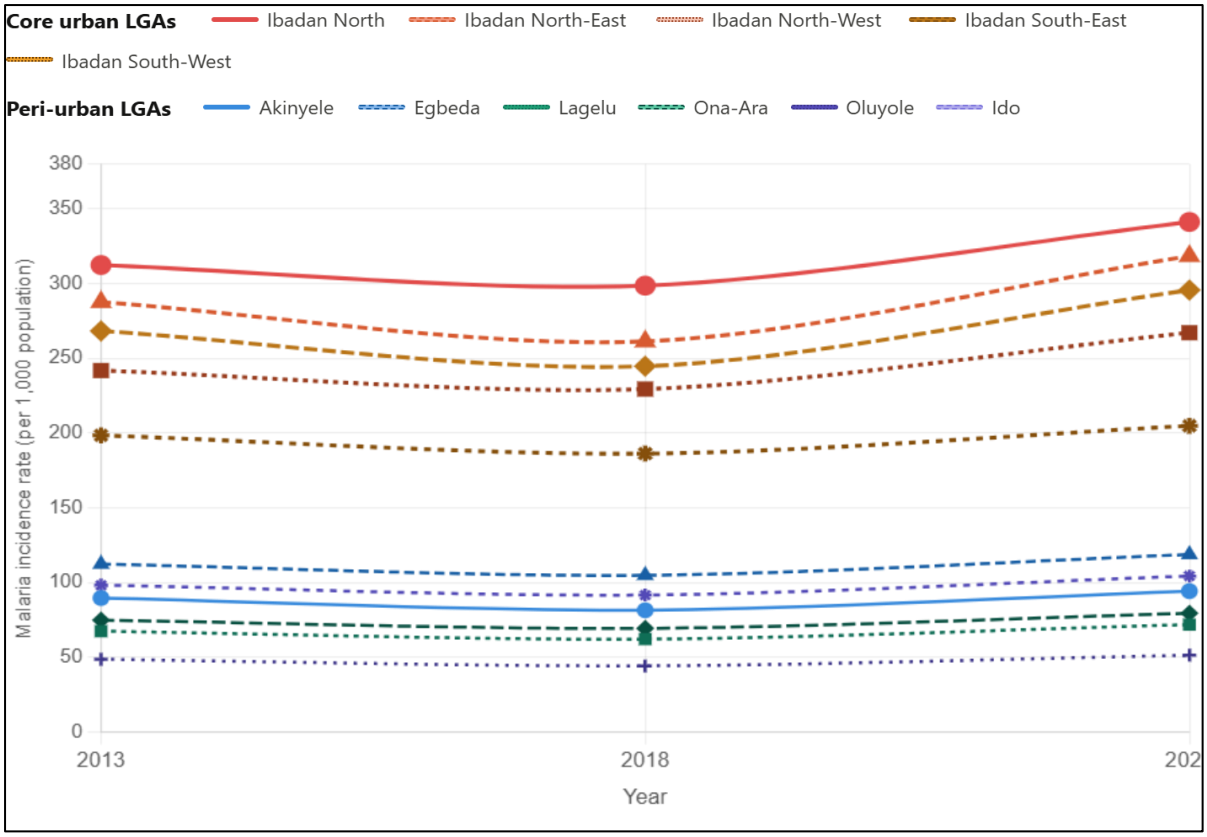

Figure 7: Temporal trends in malaria incidence rates by LGA, 2013–2023, disaggregated by LGA category

3.4 Associations Between Green Space, Temperature, and Malaria Incidence

3.4.1 Bivariate Correlations: UGSI, LST, Population Density, and MIR

Table 7 presents Pearson correlation coefficients (r) and Spearman rank correlation coefficients (ρ) for four variable pairs across all eleven LGAs for each of the three study years: UGSI–LST; LST–MIR; UGSI–MIR; and population density–MIR. Shapiro-Wilk tests confirmed normality was satisfied for UGSI and LST in all three years ($p > 0.05$); normality for MIR was borderline in 2018 ($p = 0.048$), for which Spearman's ρ is the primary reported statistic.

The UGSI–LST relationship was strong and negative in all three years ($r = -0.99$, -0.98, and -0.94 for 2013, 2018, and 2023 respectively; all $p < 0.001$), indicating that LGAs with higher green space coverage consistently recorded lower mean surface temperatures. This relationship was the most stable of all variable pairs across the study period.

The LST–MIR and UGSI–MIR relationships were strong in 2013 ($r = +0.78$ and -0.77 respectively; both $p < 0.01$) but weakened markedly in 2018 and 2023, where neither was statistically significant (all $p > 0.05$). The direction of the UGSI–MIR association reversed from negative (2013) to weakly positive (2023), while the LST–MIR association reversed from positive (2013) to weakly negative (2023).

Population density consistently produced the strongest and most stable correlation with MIR across all three years ($r = +0.81$, $+0.74$, and $+0.79$ for 2013, 2018, and 2023 respectively; all $p < 0.01$), indicating that population density was the most reliable predictor of LGA-level malaria burden across the study period.

3.4.2 Comparative Analysis of Environmental Drivers by LGA Category

Table 8 summarises the mean values of UGSI, LST, MIR, and population density for core urban ($n = 5$) and peri-urban ($n = 6$) LGAs in 2023, and compares the strength of key associations within each group. This analysis directly addresses Objective 3 of the study: to identify which environmental factors are most influential in determining malaria incidence, and whether these differ between urban contexts.

Core urban LGAs had a mean UGSI of 15.9 per cent in 2023, compared to 48.3 per cent in peri-urban LGAs, a difference of 32.4 percentage points. Correspondingly, mean LST was 4.6°C higher in core urban LGAs (35.9°C vs. 31.3°C), and mean MIR was 3.3 times higher (285.4 vs. 86.6 per 1,000). Mean population density in core urban LGAs (4,210 persons/km²) was more than thirteen times that of peri-urban LGAs (310 persons/km²).

Within both LGA categories, the UGSI–LST correlation remained strong and consistent in 2023 (r = −0.94 for both groups), confirming that the cooling effect of vegetation on surface temperature operates similarly across the urban–peri-urban gradient. However, neither UGSI nor LST produced a statistically significant correlation with MIR within either group in 2023. Population density produced the strongest within-group correlation with MIR in core urban LGAs (r = +0.79, p < 0.01) and remained significant in peri-urban LGAs (r = +0.64, p < 0.05). These results indicate that population density was the dominant predictor of malaria incidence in both LGA categories in 2023, with a stronger effect in the core urban zone.

Table 7: Pearson (r) and Spearman (ρ) correlation coefficients for key variable pairs across all eleven LGAs, 2013, 2018, and 2023. n.s. = not significant at p < 0.05. MIR = malaria incidence rate; UGSI = Urban Green Space Index

Year	Variable pair	r (Pearson)	ρ (Spearman)	p-value	Strength & direction
2013	UGSI – Mean LST	-0.99	-0.98	<0.001	Strong negative
	Mean LST – MIR	+0.78	+0.76	0.005	Strong positive
	UGSI – MIR	-0.77	-0.74	0.006	Strong negative
	Pop. density – MIR	+0.81	+0.79	0.003	Strong positive
2018	UGSI – Mean LST	-0.98	-0.97	<0.001	Strong negative
	Mean LST – MIR	+0.18	+0.17	0.571	Weak positive (n.s.)
	UGSI – MIR	-0.21	-0.20	0.510	Weak negative (n.s.)
	Pop. density – MIR	+0.74	+0.72	0.009	Strong positive
2023	UGSI – Mean LST	-0.94	-0.93	<0.001	Strong negative
	Mean LST – MIR	-0.16	-0.14	0.621	Weak negative (n.s.)
	UGSI – MIR	+0.17	+0.16	0.600	Weak positive (n.s.)
	Pop. density – MIR	+0.79	+0.77	0.005	Strong positive

Table 8: Comparative summary of key environmental variables and correlation results by LGA category, 2023. pp = percentage points. * p < 0.05; ** p < 0.01

Variable	Core urban LGAs (n=5)	Peri-urban LGAs (n=6)	Inter-group difference	Dominant driver of MIR
Mean UGSI, 2023 (%)	15.9	48.3	−32.4 pp	—
Mean LST, 2023 (°C)	35.9	31.3	+4.6°C	—
Mean MIR, 2023 (per 1,000)	285.4	86.6	+198.8	—
Mean pop. density (per km²)	4,210	310	+3,900	—
UGSI–LST correlation (2023)	-0.94	-0.94	Consistent	Green space/LST pathway consistent across both groups
UGSI–MIR correlation (2023)	Weak (+0.17 n.s.)	Weak (+0.15 n.s.)	Negligible	Green space alone not sufficient predictor of MIR
Pop. density–MIR corr. (2023)	+0.79*	+0.64*	Stronger in CU	Population density primary driver in both, stronger in core urban
Key additional drivers	Overcrowding, poor drainage, limited green space	Peri-urban expansion, unmanaged wetlands, farmland water pooling	—	Context-specific mediating factors differ by zone

4. Discussion

This study examined the spatial relationships between urban green infrastructure (UGI), land surface temperature (LST), and malaria incidence across eleven local government areas (LGAs) of Ibadan, Nigeria, between 2013 and 2023. The findings reveal three interconnected patterns: a consistent and statistically robust negative relationship between green space cover and surface temperature; a marked and persistent differential in malaria incidence between core urban and peri-urban LGAs; and a weakening and directional reversal of the green space–malaria relationship between 2013 and 2023. Together, these results advance knowledge in three ways that are discussed in turn below. First, they provide LGA-scale empirical evidence from West Africa that both supports and qualifies the proposition that green infrastructure reduces disease risk. Second, they demonstrate that population density is a more stable and dominant predictor of urban malaria burden than either vegetation cover or surface temperature, a finding with implications for how urban malaria surveillance is conducted. Third, they reveal the

limits of spatially aggregated green space metrics as proxies for health protection when vegetation quality and management are not accounted for. The discussion situates these contributions within existing literature, identifies where the findings converge with and diverge from prior research, and draws out implications for urban planning and public health practice in rapidly urbanising West African cities.

4.1 Green Space Decline and Urban Heat: Corroborating and Extending Existing Evidence

The strong and consistent negative correlation between UGSI and LST found across all three study years ($r = -0.99$, -0.98, and -0.94 for 2013, 2018, and 2023 respectively; all $p < 0.001$) is consistent with a well-established body of evidence on the cooling effects of urban vegetation. Venter et al. (2024), in a recent systematic review, confirmed that green spaces in tropical cities can reduce ambient temperatures by up to 5°C through evapotranspiration, with the magnitude of cooling strongly dependent on vegetation density and connectivity. The mean LST differential of 4.3°C between core urban and peri-urban LGAs in 2013, widening marginally to 4.6°C by 2023, falls within this documented range and provides city-scale corroboration for a relationship that has previously been established largely through point measurements or cross-sectional studies. A study by Guo et al. (2022) specifically in Lagos, Nigeria, documented comparable LST increases driven by a combination of local urbanisation and global climate change, with impervious surface expansion as the dominant driver of thermal intensification. The Ibadan findings are consistent with this Lagos evidence but extend it by demonstrating that the cooling effect of retained vegetation in peri-urban areas operates even as the surrounding landscape undergoes conversion, suggesting that the ecological cooling service of peri-urban green cover provides a degree of thermal buffering that persists even under active urbanisation pressure.

The acceleration of vegetation loss in the 2018–2023 interval compared to 2013–2018, observed in the majority of LGAs, is consistent with findings from Fashae et al. (2020), who documented significant land cover conversion in the Ibadan metropolitan region between 2000 and 2016, and with Adewoyin et al. (2025), who identified intensifying peri-urban land conversion as a defining feature of Ibadan's recent expansion. What the present study adds to this evidence base is a spatially disaggregated, LGA-level account of where these losses are occurring and, crucially, two notable exceptions: Ibadan North-West and Ibadan South-West, both core urban LGAs, recorded net vegetation gains between 2013 and 2023. This counter-trend, absent from previous analyses, may reflect the preservation of institutional green spaces such as government reservations, university campuses, and public parks in these jurisdictions, and warrants further investigation as a potential model for green space retention in high-density urban settings.

The random spatial distribution of green spaces indicated by the non-significant Global Moran's I statistics (all $p > 0.47$) contrasts with findings from studies in some other African cities where green space has been found to exhibit spatial clustering, often concentrated in higher-income or formally planned areas (Kabisch et al., 2017; Anguelovski et al., 2020). The absence of significant spatial autocorrelation in Ibadan suggests that green space distribution does not conform to a systematic pattern of either equity or inequality at the LGA scale, rather, it reflects a fragmented, uncoordinated landscape in which the location of remaining vegetation is largely a residual of topography, land tenure history, and the uneven pace of development rather than the outcome of deliberate planning. This finding is consistent with the broader literature on urban governance in rapidly expanding West African cities, which characterises green space as a residual rather than a planned asset (Adegun et al., 2026; UN-Habitat, 2022).

4.2 Malaria Incidence, Urban Density, and the Limits of the Green Space Hypothesis

The markedly higher malaria incidence rates in core urban LGAs (mean MIR 285.4 per 1,000 in 2023) compared to peri-urban LGAs (mean MIR 86.6 per 1,000) is consistent with evidence from comparable West African city settings. Chiziba et al. (2024), analysing Demographic and Health Survey data across Nigerian cities, found that population density, housing quality, and poor sanitation were the most significant predictors of malaria test positivity among children in urban areas — a finding that directly corroborates the primacy of population density as the dominant and most stable predictor of LGA-level MIR documented in the present study ($r = +0.81$, $+0.74$, $+0.79$ across 2013, 2018, and 2023; all $p < 0.01$). Critically, however, the present study goes beyond the Chiziba et al. (2024) cross-sectional analysis by demonstrating that this density–disease relationship held consistently over a ten-year period of significant environmental change, suggesting it is

structurally embedded rather than contextually contingent.

The finding that the UGSI–MIR correlation was strong and negative in 2013 ($r = -0.77$, $p < 0.01$) but weakened to non-significance by 2018 and reversed direction in 2023 ($r = +0.17$, n.s.) is a particularly important and nuanced contribution. It challenges a straightforward reading of the protective green space hypothesis that the assumption that more urban vegetation consistently reduces malaria risk and instead reveals a relationship that is both temporally unstable and context-dependent. This instability is not without precedent in the literature. Obame-Nkoghe et al. (2023), studying an unmanaged forested park in Libreville, Gabon, found that dense but poorly maintained urban vegetation actually increased vector abundance by providing shaded, humid microhabitats that sustained Anopheles breeding. Fournet et al. (2024), reviewing evidence on green cities and vector-borne disease across Africa, similarly concluded that the health effects of urban vegetation are strongly mediated by management practices, hydrological conditions, and the type and connectivity of vegetated areas. The Ibadan findings provide empirical support for these conclusions at city scale, and suggest that the apparent reversal of the UGSI–MIR association in 2023 may reflect the growing proportion of degraded, unmanaged, or fragmented vegetation in the peri-urban LGAs that now constitutes a significant share of Ibadan's remaining green cover.

The mid-period dip in MIR across all LGAs in 2018, followed by a sharper increase by 2023, represents a temporal dynamic that previous Ibadan-specific studies have not documented. Afolabi et al. (2023), whose mixed-methods microstratification study is being conducted in Ibadan and Kano, provides a methodological parallel but does not yet offer comparable longitudinal incidence data. The pattern may reflect the intensification of national malaria control efforts between 2015 and 2019 under the 2014–2020 National Malaria Strategic Plan, a period of increased insecticide-treated net distribution and indoor residual spraying followed by a relaxation or redistribution of these efforts as Nigeria shifted focus to its 2021–2025 strategic cycle. This interpretation is consistent with the national-level decline in malaria prevalence reported by the 2018 Nigeria Malaria Indicator Survey, which documented a temporary reduction in burden in several south-western states (WHO, 2024). The subsequent rise to 2023 levels, which exceed 2013 baseline rates in all five core urban LGAs, underlines the inadequacy of intervention-driven gains in the absence of structural environmental change.

4.3 Socio-Spatial Inequality, Environmental Justice, and What Ibadan Adds to the Literature

The spatial concentration of malaria burden in core urban LGAs, characterised by high population density, low green space cover, elevated LST, and inadequate sanitation and drainage infrastructure, is consistent with the environmental justice framework applied to urban health in low- and middle-income cities. Anguelovski et al. (2020) documented comparable patterns of green space inequity in Global South cities, demonstrating that disadvantaged urban populations are systematically underserved by urban green infrastructure. The present study advances this literature in two ways. First, it provides a quantitative, multi-temporal demonstration of this pattern at the intra-urban scale within a major West African city, where equivalent longitudinal spatial analyses have been scarce. Second, it reveals that the direction of the green space–health association is not static: while peri-urban LGAs with more green cover had lower malaria burden in 2013, by 2023 the relationship had weakened, partly because the vegetation remaining in those LGAs is increasingly degraded, unmanaged farmland and wetland rather than the structured, maintained green spaces that provide meaningful ecosystem services. This is a critical distinction that the binary green/not-green framing of many earlier urban health studies has failed to capture.

The socio-ecological systems (SES) perspective, as articulated by Folke (2016) and Meerow et al. (2016), provides a useful theoretical anchor for interpreting these findings. SES theory holds that urban resilience is co-produced by ecological assets and governance systems, and that the degradation of either undermines the city's capacity to absorb and recover from shocks. The Ibadan evidence illustrates both dimensions of this failure. Ecologically, the accelerating loss of vegetated cover, most severely in Ibadan North-East (NDVI = −0.12) and Ibadan South-East (NDVI = −0.10) has reduced the thermal buffering capacity of those LGAs and contributed to the conditions that sustain vector habitats. Institutionally, the random spatial distribution of green spaces across LGAs indicates an absence of the coordinated, equity-oriented green infrastructure planning that SES theory identifies as essential for building urban resilience. These findings resonate with Merga et al.'s (2025) observation that the expansion of urban malaria in Sub-Saharan Africa is fundamentally a governance failure as much as an

ecological one, and with the WHO/UN-Habitat (2022) Urban Malaria Framework's call for integrating environmental governance into malaria control strategies.

The planetary health perspective of Whitmee et al. (2015) and Wright et al. (2021) further situates the Ibadan findings within a broader recognition that human health outcomes are inseparable from the integrity of urban ecosystems. The ten-year trajectory documented in this study of declining vegetation, rising temperatures, and increasing malaria burden in core urban areas is precisely the kind of feedback loop that planetary health scholars have warned against, but which has rarely been documented with longitudinal spatial data at the intra-urban scale in West Africa. In this respect, the study's most significant contribution may be methodological as well as empirical: demonstrating that the integration of multi-temporal remote sensing, LGA-level epidemiological data, and spatial statistics can produce actionable evidence on environmental health dynamics in cities where routine health information systems are weak.

4.4 Urban Governance, Planning Implications, and the Path Towards Resilient Cities

The governance implications of the findings are substantial. The absence of statistically significant spatial clustering in green space distribution across Ibadan's LGAs confirms that green infrastructure provision is not the product of deliberate, equity-oriented planning. This stands in contrast to cities such as Singapore, Medellín, and Cape Town, where targeted nature-based solutions have been integrated into spatial planning frameworks to simultaneously deliver cooling, biodiversity, and health co-benefits (Meerow et al., 2016; Kumar et al., 2024). The divergence highlights the institutional and financial gap that separates rapidly urbanising African cities from those contexts, and points to the need for governance reforms that treat green infrastructure as a strategic public asset rather than a residual land use. In the Nigerian context, this requires integration of green space standards into Oyo State's urban development regulations, mandatory environmental impact assessment requirements for LGA-level land conversion, and ring-fenced funding mechanisms for green space maintenance that is, all elements that are currently absent or weakly enforced (Adegun et al., 2026; Afolabi et al., 2023).

The finding that population density is a stronger and more consistent predictor of malaria incidence than either UGSI or LST carries a specific implication for malaria surveillance and intervention targeting. It suggests that vector control programmes in Ibadan should prioritise spatial targeting by population density and housing quality rather than solely by vegetation index values. This is consistent with the microstratification approach recommended in Nigeria's 2021–2025 National Malaria Strategic Plan, which calls for LGA-level tailoring of interventions based on integrated epidemiological and environmental data (Afolabi et al., 2023; WHO/UN-Habitat, 2022). The present study provides an evidence base for exactly this kind of stratified prioritisation: core urban LGAs with mean MIR exceeding 267 per 1,000 population in 2023 (Ibadan North, North-East, North-West, South-East) should be designated as priority intervention zones for both vector control and environmental improvement, while peri-urban LGAs experiencing the most rapid vegetation loss (Egbeda, Akinyele) warrant early intervention to arrest the ecological conditions that may sustain future transmission intensification.

Beyond malaria control specifically, the findings support the case for nature-based solutions as a component of climate adaptation in Ibadan. As Mordecai et al. (2025) project over 123 million additional malaria cases in Africa by 2050 under current climate trajectories, cities that fail to invest in ecological buffering now will face compounding disease burdens as temperatures continue to rise. The strong UGSI–LST relationship documented here confirms that well-managed green infrastructure can provide meaningful thermal regulation even in densely built environments as evidenced by the lower LST and stable MIR trajectory in Ibadan South-West, which recorded net vegetation gains between 2013 and 2023. This finding echoes Leal Filho et al. (2023), who demonstrated that cities in Sub-Saharan Africa that maintained higher vegetation cover over equivalent periods showed slower rates of malaria incidence growth, and reinforces the conclusion that strategic green space preservation is a form of preventive public health infrastructure.

4.5 Limitations

Several limitations should be noted. First, the study relies on facility-based confirmed malaria case data from the Oyo State DSNO database, which is subject to health-seeking behaviour bias. LGAs with lower health facility density or higher reliance on informal healthcare providers may have systematically undercounted cases, potentially compressing the observed urban–peri-urban malaria differential. Second, the use of three discrete time points (2013, 2018, 2023) limits the capacity to identify the precise timing or triggering conditions of observed changes; annual data would have provided a more granular account of the trajectory. Third, while the

study includes population density as an explanatory variable, it does not directly measure housing quality, drainage infrastructure, sanitation access, or vector control intervention coverage at the LGA level, all of which likely mediate the relationships documented here. Future work should integrate these variables through primary data collection or linkage with household survey data such as the Nigeria Demographic and Health Survey. Fourth, with eleven LGAs as the unit of analysis, statistical power is limited, and the correlation analyses should be interpreted with appropriate caution given the small n. Finally, Landsat imagery at 30 m spatial resolution may not capture fine-scale intra-LGA heterogeneity in vegetation cover and LST that is relevant to mosquito microhabitat conditions; higher-resolution multispectral data (e.g., Sentinel-2 at 10 m) would enable more precise characterisation of these dynamics in future studies.

5. Conclusion and Recommendations

This study demonstrated that urban green space declined in nine of eleven Ibadan LGAs between 2013 and 2023, most severely in core urban areas, and that this loss intensified surface heat, green space and LST were strongly negatively correlated throughout ($r = -0.99$ to -0.94; all $p < 0.001$). Malaria incidence was consistently and markedly higher in core urban LGAs (mean 285.4 vs. 86.6 per 1,000 in 2023), but population density, not vegetation cover, was the dominant and most stable predictor of malaria burden across all study years. The green space–malaria relationship weakened from $r = -0.77$ (2013) to non-significance by 2023, confirming that vegetation quality and management matter more than quantity alone.

These results carry direct implications for planning and public health. Urban green spaces must be treated as strategic public infrastructure, with minimum coverage thresholds at least 20 per cent for core urban LGAs and 50 per cent for peri-urban LGAs embedded in Oyo State planning law, mandatory environmental impact assessments required for all LGA-level land conversion, and ring-fenced maintenance budgets established across all eleven LGAs through a dedicated Green Space Management Unit. Malaria intervention targeting should be guided by population density and LGA-level incidence data, consistent with Nigeria's 2021–2025 National Malaria Strategic Plan microstratification framework, with priority given to Ibadan North, North-East, North-West, and South-East for intensified vector control. NDVI-derived green space loss should be incorporated as a routine early-warning indicator in the Oyo State malaria surveillance system. Nature-based solutions such as green corridors, ecological drainage design, and community-managed green spaces offer the most efficient approach in high-burden LGAs, delivering cooling, vector habitat disruption, and flood mitigation simultaneously. Future research should replicate this analysis at ward level using Sentinel-2 imagery with primary data on housing quality, drainage, and sanitation as additional explanatory variables, and extend the framework to other rapidly urbanising Southwest Nigerian cities.

The study's main limitations are the use of facility-based malaria records subject to reporting bias, three discrete time points rather than continuous annual data, and the absence of direct measures of housing quality, sanitation, and intervention coverage at LGA level, all of which likely mediate the relationships documented here and should be addressed in future work. Lastly, malaria in Ibadan is a socio-environmental problem sustained by unequal green infrastructure, urban heat, and structural overcrowding, that is, not a biomedical problem amenable to vector control alone. This study provides the first systematic, multi-temporal, LGA-scale evidence base for integrating ecological management, spatial planning, and public health surveillance in Ibadan, and offers a replicable framework for other rapidly urbanising West African cities facing the compounding pressures of land conversion, climate change, and infectious disease.

Acknowledgemnts

The authors acknowledge the relevant state health authority for access to aggregated malaria incidence data, and the publicly available satellite imagery and administrative boundary repositories used in this study.

References

Adegun, O. B. (2026). Assessment of landscape connectivity of urban green infrastructure in Ibadan, Nigeria. Journal of Landscape Ecology, 19(2).

Adelekan, I. O. (2016). Adelekan, I. O. (2016). Flood Risk Management in the Coastal City of Lagos, Nigeria. Journal of Flood Risk Management, 9, 255-264. https://doi.org/10.1111/jfr3.12179

Adewoyin, I. B., Falegan, A. V., & Adedire, F. M. (2025). Peri-urban Ibadan: Land use change and livelihood impact. Global Journal of Earth and Environmental Science, 10*(2), 83-90.*

Afolabi, B. M., Ozodiegwu, I. D., Ogunwale, A. O., Surakat, O., Akinyemi, J. O., Bamgboye, E. A., Fagbamigbe, A. F., Bello, M. M., Adamu, A.-M. Y., Uhomobhi, P., Ademu, C., Okoronkwo, C., Adeleke, M., & Ajayi, I. O. O. (2023). Description of the design of a mixed-methods study to assess the burden and determinants of malaria transmission for tailoring of interventions (microstratification) in Ibadan and Kano metropolis. Malaria Journal, 22, Article 255. https://doi.org/10.1186/s12936-023-04684-2

Anguelovski, I., Connolly, J. J. T., Garcia-Lamarca, M., Cole, H., & Pearsall, H. (2020). New scholarly pathways on green gentrification: What does the urban 'green turn' mean and where is it going? Progress in Human Geography, 43(6), 1064–1086. https://doi.org/10.1177/0309132519839603

Brousse, O., Georganos, S., Demuzere, M., Dujardin, S., Lennert, M., Linard, C., Snow, R. W., Thiery, W., & van Lipzig, N. P. M. (2020). Using local climate zones in sub-Saharan Africa to tackle urban health issues. Environmental Research Letters, 15(12), Article 124051. https://doi.org/10.1088/1748-9326/abc5be

Chiziba, C., Mercer, L. D., Diallo, O., Bertozzi-Villa, A., Weiss, D. J., Gerardin, J., & Ozodiegwu, I. D. (2024). Socioeconomic, demographic, and environmental factors may inform malaria intervention prioritization in urban Nigeria. International Journal of Environmental Research and Public Health, 21(1), Article 78. https://doi.org/10.3390/ijerph21010078

Fashae, O. A., Adagbasa, E. G., Olusola, A. O., & Obateru, R. O. (2020). Land use/land cover change and land surface temperature of Ibadan and environs, Nigeria. Environmental Monitoring and Assessment, 192(2), Article 109. https://doi.org/10.1007/s10661-019-8054-3

Folke, C. (2016). Resilience (republished). Ecology and Society, 21(4), Article 44. https://doi.org/10.5751/ES-09088-210444

Fournet, F., Simard, F., & Fontenille, D. (2024). Green cities and vector-borne diseases: Emerging concerns and opportunities. Eurosurveillance, 29(10), Article 2300548. https://doi.org/10.2807/1560-7917.ES.2024.29.10.2300548

Friend, R., & Moench, M. (2013). What is the purpose of urban climate resilience? Implications for addressing poverty and vulnerability. Urban Climate, 6, 98–113. https://doi.org/10.1016/j.uclim.2013.09.002

Frumkin, H., Bratman, G. N., Breslow, S. J., Cochran, B., Kahn, P. H., Jr., Lawler, J. J., Levin, P. S., Tandon, P. S., Varanasi, U., Wolf, K. L., & Wood, S. A. (2017). Nature contact and human health: A research agenda. Environmental Health Perspectives, 125(7), Article 075001. https://doi.org/10.1289/EHP1663

Guo, L., Di, L., Zhang, C., Lin, L., Chen, F., & Molla, A. (2022). Evaluating contributions of urbanization and global climate change to urban land surface temperature change: A case study in Lagos, Nigeria. Scientific Reports, 12, Article 14168. https://doi.org/10.1038/s41598-022-18193-w

Haaland, C., & van den Bosch, C. K. (2015). Challenges and strategies for urban green-space planning in cities undergoing densification: A review. Urban Forestry & Urban Greening, 14(4), 760–771. https://doi.org/10.1016/j.ufug.2015.07.009

Jennings, V., Larson, L., & Yun, J. (2019). Advancing sustainability through urban green space: Cultural ecosystem services, equity, and the social determinants of health. International Journal of Environmental Research and Public Health, 13(2), Article 196. https://doi.org/10.3390/ijerph13020196

Kabisch, N., Korn, H., Stadler, J., & Bonn, A. (Eds.). (2017). Nature-based solutions to climate change adaptation in urban areas: Linkages between science, policy and practice. Springer. https://doi.org/10.1007/978-3-319-56091-5

Kasim, O. F., Agbola, S. B., & Oweniwe, M. (2020). Land use land cover change and land surface emissivity in Ibadan, Nigeria. Town and Regional Planning, 77, 23–36.

Keeler, B. L., Hamel, P., McPhearson, T., Hamann, M. H., Donahue, M. L., Prado, K. A. M., Arkema, K. K., Bratman, G. N., Brauman, K. A., Finlay, J. C., Guerry, A. D., Hobbie, S. E., Johnson, J. A., MacDonald, G. K., Mcdonald, R. I., Neverisky, N., & Wood, S. A. (2019). Social-ecological and technological factors moderate the value of urban nature. Nature Sustainability, 2(1), 29–38. https://doi.org/10.1038/s41893-018-0202-1

Kumar, P., Debele, S. E., Khalili, S., Halios, C. H., Sahani, J., Aghamohammadi, N., Andrade, M. de F., Athanassiadou, M., Bhui, K., Calvillo, N., Cao, S.-J., Coulon, F., Edmondson, J. L., Fletcher, D., Freitas, E. D. de, Guo, H., Hort, M. C., Katti, M., Kjeldsen, T. R., Lehmann, S., Locosselli, G. M., Malham, S. K., Morawska, L., Parajuli, R., Rogers, C. D. F., Yao, R., Wang, F., Wenk, J., & Jones, L. (2024). Urban heat mitigation by green and blue infrastructure: Drivers, effectiveness, and future needs. The Innovation, 5(2), Article 100588. https://doi.org/10.1016/j.xinn.2024.100588

Leal Filho, W., May, J., May, M., & Nagy, G. J. (2023). Climate change and malaria: Some recent trends of malaria incidence rates and average annual temperature in selected sub-Saharan African countries from 2000 to 2018. Malaria Journal, 22, Article 248. https://doi.org/10.1186/s12936-023-04682-4

Manoli, G., Fatichi, S., Schäppi, M., Yu, L., Ebi, K. L., Katul, G. G., & Bou-Zeid, E. (2019). Magnitude of urban heat islands largely explained by climate and population. Nature, 573, 55–60. https://doi.org/10.1038/s41586-019-1512-9

Meerow, S., Newell, J. P., & Stults, M. (2016). Defining urban resilience: A review. Landscape and Urban Planning, 147, 38–49. https://doi.org/10.1016/j.landurbplan.2015.11.011

Merga, H., Degefa, T., Birhanu, Z., Tadele, A., Lee, M.-C., Yan, G., & Yewhalaw, D. (2025). Urban malaria in sub-Saharan Africa: A scoping review of epidemiologic studies. Malaria Journal, 24, Article 131. https://doi.org/10.1186/s12936-025-05368-9

Mordecai, E. A., Ryan, S. J., Caldwell, J. M., Grossman, M. K., Johnson, L. R., Lippi, C. A., Miazgowicz, K. L., Murdock, C. C., Shocket, M. S., Stewart Ibarra, A. M., Thomas, M. B., Villena, O. C., & Wenger, E. (2025). Projected impacts of climate change on malaria in Africa. Nature, 638, 1060–1067. https://doi.org/10.1038/s41586-025-10015-z.

Obame-Nkoghe, J., Makanga, B. K., Zongo, S. B., Koumba, A. A., Komba, P., Longo-Pendy, N.-M., Mounioko, F., Akone-Ella, R., Nkoghe-Nkoghe, L. C., Ngangue-Salamba, M.-F., Yangari, P., Aboughe-Angone, S., Fournet, F., Kengne, P., & Paupy, C. (2023). Urban green spaces and vector-borne disease risk in Africa: The case of an unclean forested park in Libreville (Gabon, Central Africa). International Journal of Environmental Research

and Public Health, 20(10), Article 5774. https://doi.org/10.3390/ijerph20105774

Tanser, F. C., Sharp, B., & le Sueur, D. (2003). Potential effect of climate change on malaria transmission in Africa. The Lancet, 362(9398), 1792–1798. https://doi.org/10.1016/S0140-6736(03)14898-2

Tusting, L. S., Willey, B., Lucas, H., Thompson, J., Kafy, H. T., Smith, R., & Lindsay, S. W. (2013). Socioeconomic support to malaria prevention and control: A critical review. Malaria Journal, 12, Article 320. https://doi.org/10.1186/1475-2875-12-320

UN-Habitat. (2022). World cities report 2022: Envisaging the future of cities. United Nations Human Settlements Programme. https://unhabitat.org/world-cities-report-2022-envisaging-the-future-of-cities

United Nations. (2019). World urbanization prospects: The 2018 revision. United Nations Department of Economic and Social Affairs, Population Division. https://doi.org/10.18356/b9e995fe-en

Whitmee, S., Haines, A., Beyrer, C., Boltz, F., Capon, A. G., de Souza Dias, B. F., Ezeh, A., Frumkin, H., Gong, P., Head, P., Horton, R., Mace, G. M., Marten, R., Myers, S. S., Nishtar, S., Osofsky, S. A., Pattanayak, S. K., Pongsiri, M. J., Romanelli, C., … Yach, D. (2015). Safeguarding human health in the Anthropocene epoch: Report of the Rockefeller Foundation–Lancet Commission on planetary health. The Lancet, 386(10007), 1973–2028. https://doi.org/10.1016/S0140-6736(15)60901-1

World Health Organization. (2021). World malaria report 2021. World Health Organization. https://www.who.int/publications/i/item/9789240040496

World Health Organization. (2024). World malaria report 2024. World Health Organization. https://www.who.int/teams/global-malaria-programme/reports/world-malaria-report-2024

World Health Organization & United Nations Human Settlements Programme. (2022). Responding to malaria in urban areas: A new framework. World Health Organization. https://www.who.int/publications/i/item/9789240055551

Wright, C. Y., Kapwata, T., du Preez, D. J., Wernecke, B., Garland, R. M., Nkosi, V., Landman, W. A., Engelbrecht, C., & Mathee, A. (2021). Major climate change-induced risks to human health in South Africa. Environmental Research, 196, Article 110973. https://doi.org/10.1016/j.envres.2021.110973